Increasing Recyclability of PC, ABS and PMMA: Morphology and Fracture Behavior of Binary and Ternary Blends

Jan Rybnicek,[1] Ralf Lach,[2,3] Monika Lapcikova,[4] Josef Steidl,[1] Zdenek Krulis,[4] Wolfgang Grellmann,[2] Miroslav Slouf[4]

[1]*Czech Technical University in Prague, Department of Materials Engineering, Prague, Czech Republic*
[2]*Martin-Luther University Halle-Wittenberg, Centre of Engineering, Halle (Saale), Germany*
[3]*Vienna University of Technology, Institute of Materials Science and Technology, Vienna, Austria*
[4]*Institute of Macromolecular Chemistry, Academy of Sciences of the Czech Republic, v. v. i., Prague, Czech Republic*

Received 7 December 2007; accepted 6 March 2008
DOI 10.1002/app.28376
Published online 23 May 2008 in Wiley InterScience (www.interscience.wiley.com).

ABSTRACT: Binary and ternary blends of PC, ABS, and PMMA were studied. The blends were produced from original and recycled materials by melt mixing in a wide range of compositions. Instrumented Charpy impact testing, tensile testing, rheology investigations, and electron microscopy were carried out to determine the relationship between the deformation and fracture behavior, blend composition, morphology, and processing parameters. Resistance against unstable crack propagation was evaluated using the concepts of *J*-integral and crack-tip-opening displacement (CTOD). The transition from ductile elastic-plastic to brittle-linear elastic fracture behavior was observed in the case of PC/ABS/PMMA blend at 10% of PMMA. Reprocessing had only a slight influence on the deformation and fracture behavior of the recycled blends. The blends produced from recycled materials proved to be competitive with the original pure materials. © 2008 Wiley Periodicals, Inc. J Appl Polym Sci 109: 3210–3223, 2008

Key words: ternary amorphous blends; recycling; toughness; rheology; structure–property relations

INTRODUCTION

Generally, there are two main reasons why plastics in the automotive industry need to be recycled. First, there is pressure from car manufactures on their suppliers to cut production and material costs. Second, but of great importance, is the effort to decrease the impact of end-of-life vehicles (ELV) on the environment (e.g., Directive 2000/53/EC of the EU parliament). The main restriction on broader utilization of mechanical/material recycling procedures for plastics in the automotive industry (production waste or end-of-life cars) is the fact that the car components are often composed of several plastic parts that are hard to dismantle. Separating the material demands high investment in machinery, and the operating costs are high in relation to relatively low productivity. Another problem with the separating procedures is their low efficiency: in practice, not more than 95% purity of the separated fraction is achieved.

Car rear lights offer an illustrative example from practice. They are a source of high quality engineering thermoplastics, e.g., PC, ABS, PC/ABS, and PMMA. Furthermore, if these materials are mechanically recycled, they retain their properties well, and it has become common practice to add 10–20% of the finely separated production scrap (regrind) to the original (virgin) material in a closed loop recycling process. However, production waste recycling has been limited to well separated mono-material fractions. Moreover, rear light assemblies consisting of several plastic parts (e.g., PMMA + PC, PMMA + PC/ABS, PMMA + ABS; compositions depending on the producer) are commonly disposed of in landfills or incinerated. A similar problem arises when end-of-life cars are recycled. Dismantling complicated assemblies into pure material fractions limits the economic viability of the recycling process. Recovery options for front and rear lights from end-of-life vehicles can be found, for example, in refs.[1–5]

These problems of separation are solved when the plastic waste is recycled as a multimaterial mixture. Then, a primary condition for the economic practicability of the recycling process is that the recyclate should have a high level of final utilizable properties. In this respect, a blending technology has been shown to improve the properties of recycled materials.[6–10] For example, in the work of Liu and Berlitson[6] the toughness of recycled materials was

Correspondence to: J. Rybnicek (jan.rybnicek@fs.cvut.cz).

enhanced by blending ABS with PC/ABS and by incorporating methacrylate-butadiene-styrene core-shell impact modifier (MBS). Furthermore, it was reported that the addition of 10% of PMMA in the blend of ABS/PC(65/35) + 5 phr MBS does not depress the mechanical properties, because PMMA is mutually miscible with SAN, depending on the AN level, and is compatible with PC. Since the elongation at break and the *J*-integral increased to some extent, it was anticipated that interfacial adhesion between ABS and PC would be enhanced by adding PMMA. Additionally, recycling a ternary mixture of PMMA, ABS and PC is addressed in invention, US 5,232,986.[11] The PMMA-rich composition is claimed to consist of: 50–90% of PMMA, 50–40% of ABS, and 5–40% of PC. The authors state that, with the addition of PC, the impact strength, notch impact strength, and heat resistance are improved. Recyclates are considered to be a preferable substitute in molding compositions and are reported to exhibit properties that are practically identical with those of virgin materials. In this invention, polymer blends are prepared by conventional methods making use of an extruder or a roller compounder. Furthermore, extrusion of thermoplastic mixtures in a closed loop recycling system, especially mixtures of PC/PMMA, with the addition of a compatibilizer on the basis of MBS—methylmethacrylate–butadiene–styrene or terpolymer consisting of butadiene—is described in invention US 5,569,713.[12] Recycling quaternary mixtures of PET/ABS/PC/SBS or PET/ABS/PC/SEBS, where PET is a major component, is discussed in invention US 2004209985.[13]

The aim of this work is to characterize the toughness of binary and ternary blends based on PC, ABS, and PMMA, and to specify the optimum blend composition and processing parameters to maximize the toughness. This work also investigates the possibilities for and the limits on recycling these materials as a ''multi-polymer mixture'' with the use of blending technology. In addition, instrumented Charpy impact testing, tensile testing, and rheology investigations will be carried out to determine the relationship between the deformation and fracture behavior, blend composition, morphology, and processing parameters. With regard to the toughness characterization, fracture mechanics parameters are utilized, such as *J*-integral and crack-tip-opening displacement (CTOD), measured at moderately high loading rates 1 m/s, which have been proved to provide a sensitive measure of toughness in relation to changes in morphology and microstructure.[14–16] Moreover, these parameters can be applied for a wide range of fracture behavior, from brittle linear-elastic to ductile elastic-plastic. Since the *J*-integral and CTOD relate to determining resistance to unstable crack propagation, they can be used in real structure failure assessment.

EXPERIMENTAL

Materials

The blends were produced from original and recycled materials that are used in the production of rear light assemblies: Polycarbonate PC—Lexan LS2 (GE Plastics), acrylonitrile-butadiene-styrene ABS—Cycoloy X37 (GE Plastics), poly(methyl methacrylate) PMMA—Lucryl G88 (BASF) and thermoplastic elastomer TPE (styrene-ethane/butane-styrene block copolymer)—Bergaflex BFI K70A Bergmann. The composition of binary blends was varied with a step of 25 wt %. The ternary blends were prepared with a constant PC/ABS ratio 75/25 and the content of PMMA was varied in steps of 5, 10, 25, 50 and 75 wt %. For a quaternary blend of PC/ABS + 5% PMMA + TPE, the content of TPE was kept up to 2 pph (parts per hundred).

Preparation methods

The production scrap was ground with the use of a PH TRIA 47-30/CN granulator with three rotating cutting knives. The average grind size was 5 mm. The ground material was dedusted using an Allgier dust separator, and the metal particles were detected using a Mesurtronic metal detector. The blends (original and recycled materials) were hand premixed and injection molded into Charpy specimens using a Battenfeld 500 injection molding machine. The melt and mold temperatures were kept at 245°C and 60°C, respectively. The back pressure and injection pressure were set to 10 and 130 bars. The materials were dried for a minimum of 6 h at a temperature of 105°C in a hot-air dryer.

Methods

Instrumented charpy impact testing

A minimum of 10 standardized SENB (single-edge-notched bend) specimens (ISO 179) were required for each tested material. The dimensions of the specimens were: length $L = 80$ mm, width $W = 10$ mm and thickness $B = 4$ mm. The specimens were prenotched and then an initial sharp crack of length $a = 2$ mm ($a/W = 0.2$) was produced by slow pressing a fresh razor blade into the prenotch tip. The final notch tip radius was 0.2 μm.

An instrumented Charpy impact tester ICIT-4J recorded the load—deflection (*F-f*) diagrams. The impact load was recorded with the help of strain gauges incorporated into the pendulum hammer and the data was transferred through an A/D transducer into a personal computer (see Fig. 1). The deflection of the specimen was calculated from Newton's second law of motion and also measured directly with

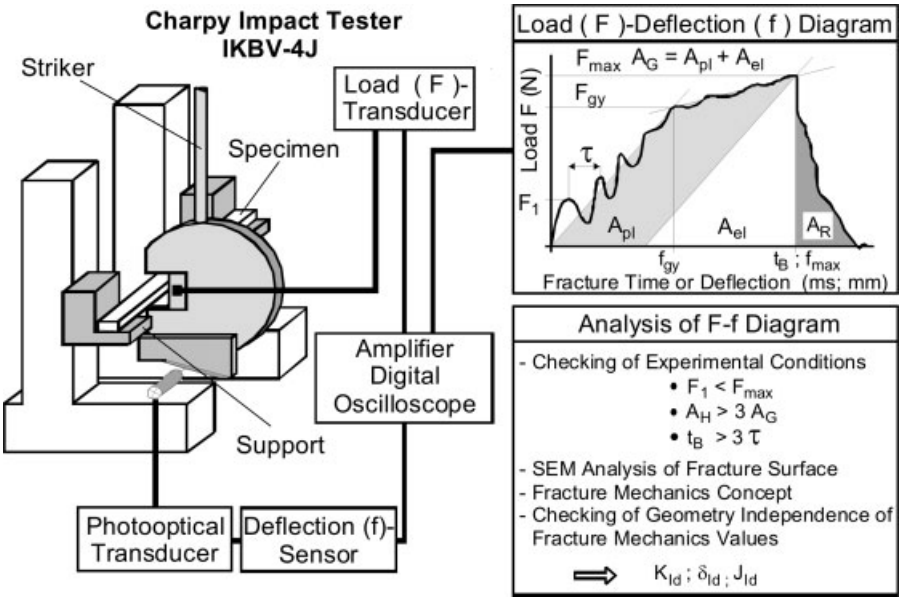

Figure 1 Scheme of instrumented Charpy impact testing device.

the help of a photo-optical system. The pendulum work capacity was 4 J (angle = 160°). The pendulum velocity reached 1.0 m/s (angle = 40°). The support span was set to s = 40 mm (s/W = 4). This set-up enabled us to determine the geometry independent fracture mechanics values.[14]

The load-deflection diagrams enabled us to determine the load and deflection at yield point (F_{gy}, f_{gy}), maximum load F_{max} and the corresponding deflection f_{max}. Elastic and plastic part of energy (A_{el}, A_{pl}) and crack propagation energy A_R were also determined. The load—deflection diagrams were acceptable if the conditions described in Figure 1 were fulfilled. After recording the load—deflection diagrams, a real value of the initial crack was measured using light microscopy. The fracture surfaces of unbroken specimens were produced by breaking specimens at a liquid nitrogen temperature and at high pendulum hammer speeds.

The dynamic flexular modulus E_d and the dynamic yield stress σ_d were calculated from the load—deflection diagrams of at least five unnotched specimens, according to the following formulas:

$$E_d = \frac{F_{gy} s^3}{4BW^3 f_{gy}} \tag{1}$$

$$\sigma_d = \frac{3F_{gy} s}{2BW^2} \tag{2}$$

The J-integral was evaluated using the method of Merkle and Corten (MC)[17]:

$$J_{Qd}^{MC} = G_I + \frac{2}{B(W-a)}[D_1 A_G + D_2 A_K - (D_1 + D_2)A_{el}] \tag{3}$$

where

$$G_I = \frac{K_I^2}{E_d}(1 - \nu^2) \tag{4}$$

is the energy release rate for a plane strain state (K_I - stress intensity factor, ν - Poisson's ratio) and

$$D_1 = \frac{1+\gamma}{1+\gamma^2} \tag{5}$$

$$D_2 = \frac{\gamma(1-2\gamma-\gamma^2)}{(1+\gamma^2)^2} \tag{6}$$

$$\gamma = \frac{1.456\ (W-a)}{s} \tag{7}$$

$$A_K = F_{max} f_{max} - A_G \tag{8}$$

$$A_G = A_{e1} + A_{pl} \tag{9}$$

The critical crack-tip-opening displacement CTOD—δ_{Qd} was determined on the basis of the plastic-hinge model[18] according to the following equation:

$$\delta_{Qd} = \frac{1}{n}(W-a)\frac{4f_{max}}{s} \tag{10}$$

where n is the rotational factor (n = 4). A modified version of CTOD - δ_{Qdk}[19,20] excludes the contribution of the unnotched specimen to deflection, and thus better describes the amount of plastic deformation in the near vicinity of the notch tip:

$$\delta_{Qdk} = \frac{1}{n}(W-a)\frac{4f_k}{s} \tag{11}$$

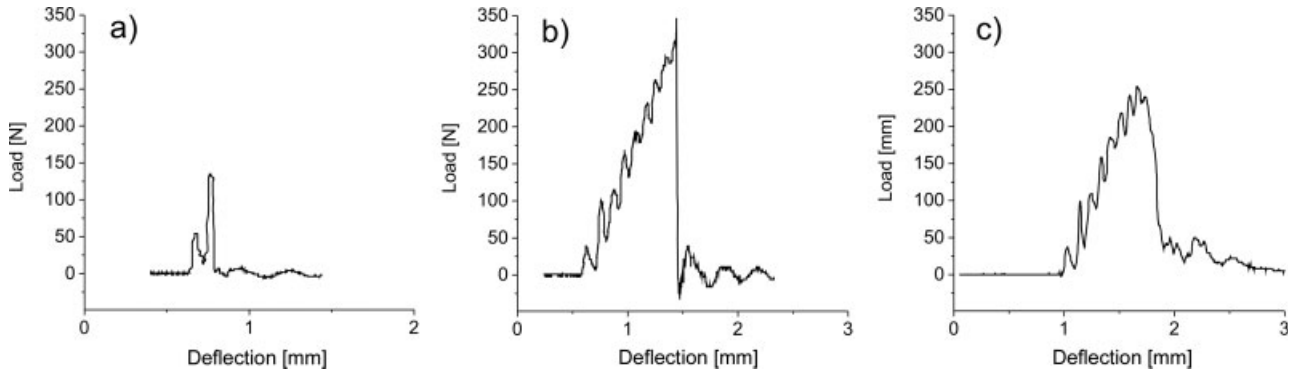

Figure 2 Load—deflection diagrams: (a) PMMA; (b) PC; (c) ABS.

$$f_k = f_{\max} - f_b \tag{12}$$

$$f_b = \frac{F_{\max} s^3}{4BW^3 E_d} \tag{13}$$

where f_b is the deflection of the unnotched part of the specimen.

Phase structure and fracture surface analysis

The smooth surfaces for the morphological study were prepared from injection molded specimens using an Ultratome III 8800 ultra-microtome (LKB-produkter AB, Sweden) equipped with a glass knife. A permanganic etching agent was used to visualize the components of the polymeric mixture. The solution of 0.35 g of $KMnO_4$ in 10 mL of sulfuric acid and 10 mL of phosphoric acid was ripened for 1 h before use. The samples were immersed into the solution for 30 s and then washed for 1 h in running water. The polymers were etched in the order PMMA, PC and polybutadiene from ABS copolymer. The impact test samples were then used for fracture surface analysis. All samples were coated with platinum (BAL-TEC SCD 050 sputter coater), and were observed with the help of a Vega TS5130 scanning electron microscope (SEM) (Tescan, CR).

Tensile testing

Yield stress σ_y and yield strain ε_y were measured using Instron 5582 tester according to ISO 527 at deformation speeds of 5 and 50 mm/min.

Rheology

Shear viscosity and shear rates were measured with the use of the Rheograf 2001 high pressure capillary viscosimeter (Goettfert) equipped with a round capillary 30.0 mm in length, 1.00 mm in diameter. The experimental data was corrected according to Rabinowitch's correction.

RESULTS AND DISCUSSION

Toughness of original materials and their binary blends

The load—deflection diagrams of PMMA, PC and ABS (Fig. 2) show fully brittle, linear-elastic behavior with unstable crack propagation (PMMA) and elastic-plastic behavior with unstable/stable crack propagation fracture behavior (PC and ABS), respectively. The J values of PC and ABS lie at the same level (Fig. 3), but the CTOD results (Fig. 4) indicate that the modified version of crack-tip-opening displace-

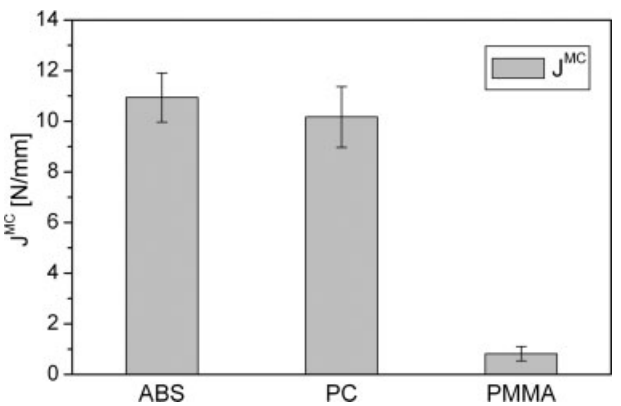

Figure 3 Results of J-values for ABS, PC and PMMA.

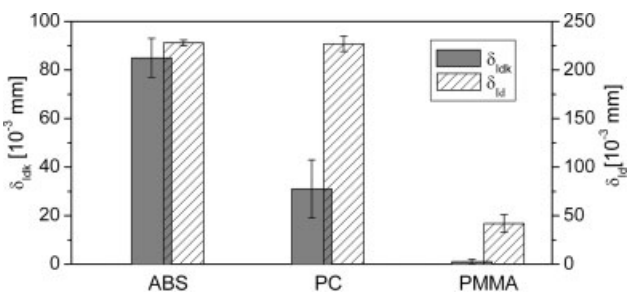

Figure 4 Results of CTOD for ABS, PC and PMMA.

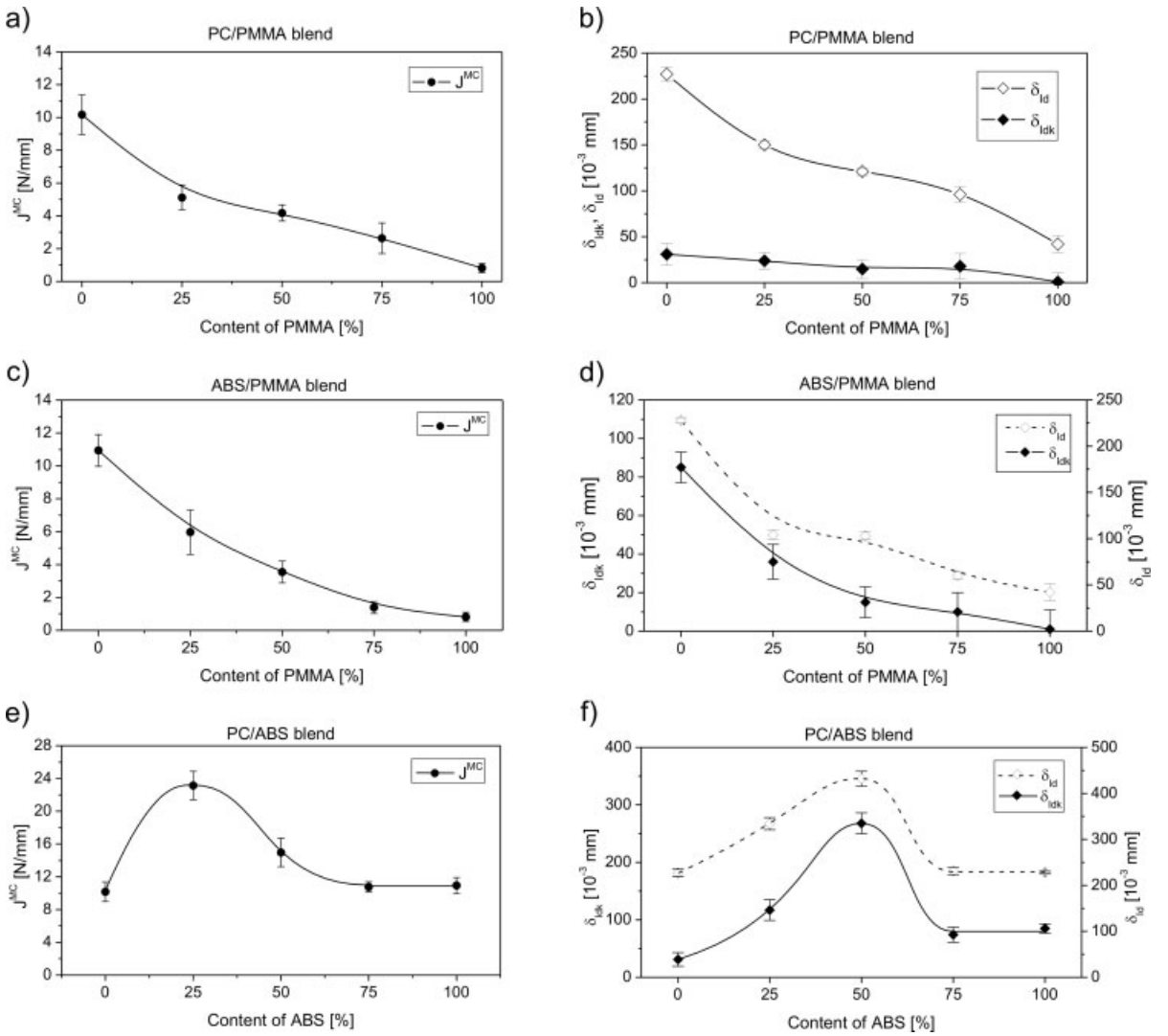

Figure 5 Toughness of binary blends: (a) *J* values of PC/PMMA; (b) CTOD of PC/PMMA; (c) *J* values of ABS/PMMA; (d) CTOD of ABS/PMMA; (e) *J* values of PC/ABS; (f) CTOD of PC/ABS.

ment δ_{Idk} is substantially higher for ABS. Both methods also indicate significant brittleness of PMMA. On the other hand, PMMA was observed to have a superior dynamic flexural modulus E_d and dynamic yield stress σ_d to PC and ABS. It was found that when PMMA is added into ABS/PMMA or PC/PMMA blend, the dynamic yield stress σ_d and the dynamic flexural modulus E_d increase almost linearly and follow the rule of mixtures (not shown here). However, the toughness of PC/PMMA and ABS/PMMA decreases with increasing content of PMMA [Fig. 5(a–d)]. In all compositions, these blends fracture in a brittle manner. This corresponds with the load—deflection diagrams, which exhibit linear elastic deformation behavior with an unstable crack growth mechanism. The *J* results show that at 25% of PMMA the toughness decreases almost by 50%; the fall in toughness is equally pronounced for both blends, but for PC/PMMA after a sharp decrease the trend levels off and continues to decline linearly. The drop in values is most obvious at 25% of PMMA, since PMMA forms a dispersed phase [Fig. 10(a,b)], thus the number of stress concentration sites is large. A similar trend in toughness deterioration (incompatibility of the blends) was found in the CTOD results [Fig. 5(b,d)]. However, plastic deformation at the initiation of unstable crack growth expressed by δ_{Idk} is considerably higher in ABS/PMMA than in PC/PMMA blend. This can be explained by the fact that δ_{Idk} of pure ABS is essentially higher than that of pure PC.

Blending PC with ABS results in a significant toughness improvement [Fig. 5(e,f)]. By adding ABS into the blend, the *J* and CTOD values are increased above those of the linear law of mixtures. Such a synergetic effect has already been well described for this composition in the literature.[21,22] The toughening is attributed to the dispersed morphology of the

ABS phase [see Fig. 10(c)], which induces plastic deformation of the PC matrix. As the content of ABS rises to 50%, the morphology turns to cocontinuous. This leads to thickening of PC matrix ligaments, where the plane stress changes to the plane strain state, resulting in less plastic deformation of PC.[21] Increasing the ABS content to 75%, the values diminish to the level of pure materials; the relatively hard PC dispersed phase cannot induce pronounced energy dissipative processes in soft ABS matrix, as is possible in the opposite case. However, in this work the maximum toughening effect was observed in the case of two different compositions. The energy determined J values indicate the maximum at ABS content of 25% [Fig. 5(e)]. In contrast, the deformation determined CTOD points to maximum values at 50% of ABS [Fig. 5(f)]. This is probably because pure ABS has distinctly higher CTOD values. The CTOD values reach their maximum at 50% ABS, but at higher contents (75% of PC) dispersed PC may act as a stress concentrator and may downgrade the plasticity of ABS. Furthermore, from the fracture surfaces and load-deflection diagrams we can see a dominant stable crack growth mechanism along the whole fracture surface and over the entire PC/ABS blend composition. The fracture surface of PC/ABS 75/25 seemed to be the most extensively plastically deformed, as was documented by the formation of shear lips (thickening of the specimen) and delaminating, which also contributed to relieving the triaxial stresses. Therefore, this composition is considered as optimal and was further utilized as a basic material combination for ternary blends with PMMA.

We were also interested in the effect of the processing parameters on the toughness of PC/ABS. It was shown by Lombardo et al.[23] that PC degrades rapidly at high temperatures when blended with ABS. PC reacts with high alkaline electrolyte and catalyst residuals from the ABS emulsion synthesis, leading to PC chain scission. In agreement with this, our investigations show that toughness depends substantially on the processing temperature (not shown here). Increasing processing temperature from 240 to 270°C resulted in 50% drop of toughness. In addition, it was found that increasing the back pressure and/or the screw speed had no improving effects. Therefore, we recommend that the thermomechanical loading of the polymer melt should be as low as possible.

Toughness of PC/ABS/PMMA ternary blend

The transition from ductile to brittle fracture behavior was observed for a PC/ABS/PMMA blend at a PMMA content of 10%. Both the J and the CTOD values indicate that the transition occurs at the same composition [Fig. 6(a,b)], where maximum scatter of the measured values can be found. The change in fracture behavior is easy to recognize in the light-microscopy images (Fig. 7). Moreover, the load—deflection diagrams show that the elastic-plastic deformation with stable crack propagation [Fig. 7(a)] turns to linear-elastic deformation with unstable crack propagation [Fig. 7(b)]. In other words, after reaching maximum force F_{max}, which is here considered to be the onset of unstable crack propagation, the crack of the ductile specimens propagates in a stable manner, in contrast to the unstable crack propagation seen in brittle specimens. Additionally, a detailed fracture surface analysis (discussed further) shows that there is also a small part of the stable crack in brittle specimens, but it is substantially reduced in comparison to ductile specimens.

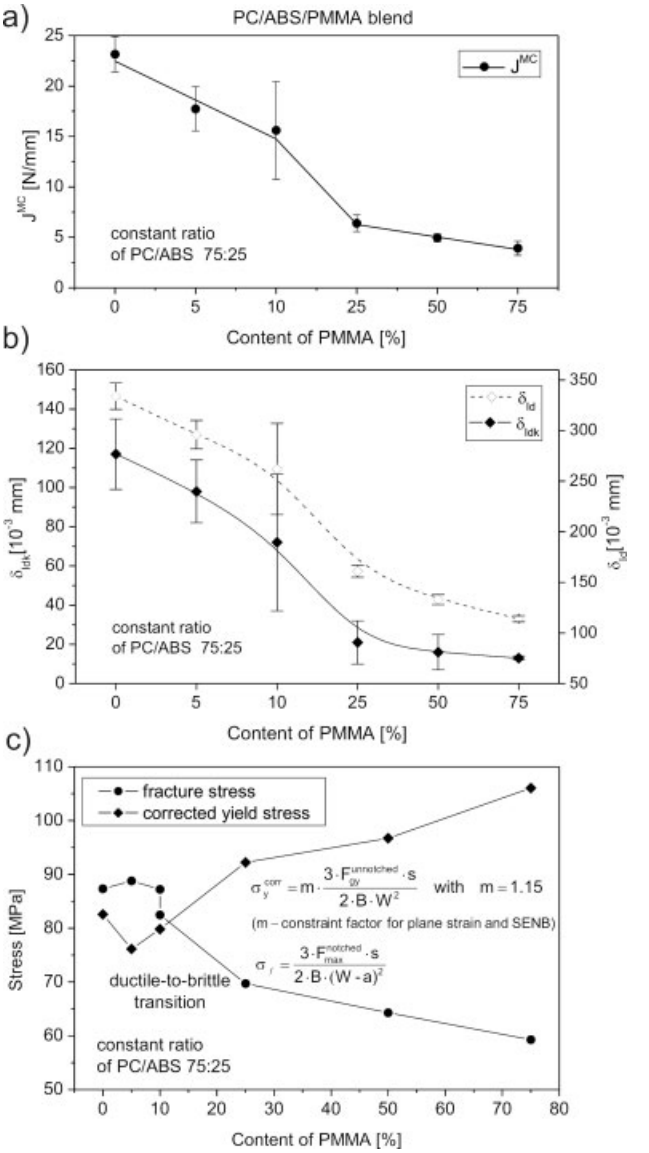

Figure 6 Toughness of ternary PC/ABS/PMMA blend: (a) J values and (b) CTOD results (c) Ductile-to-brittle transition.

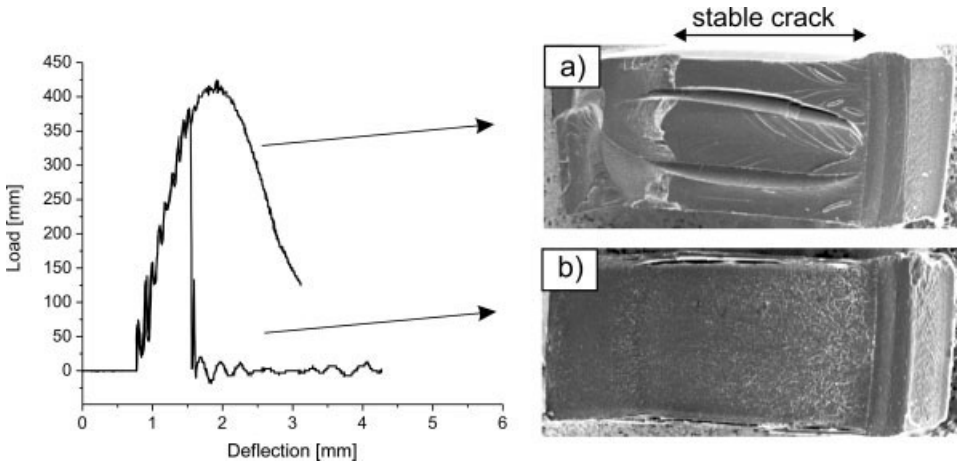

Figure 7 Ductile-to-brittle transition of PC/ABS(75/25) + 10% PMMA: Load—deflection diagram and fracture surface of (a) ductile and (b) brittle fractured specimen.

In general ductile-to-brittle transition occurs when the stress of craze initiating and the stress of shear yielding initiating are equal. Figure 6(c) shows that both the constraint-corrected yield stress σ_y^{corr} and the fracture stress σ_f, plotted versus PMMA weight fraction, are equal at about 12% PMMA. That is very close to 10% PMMA from fracture mechanics analysis in Figure 6(a,b). It has to be noted that σ_y^{corr} is approximately identical to the stress for initiating shear yielding and σ_f is only little higher than the stress for craze initiation in the brittle fracture mode.

Fracture surface analysis

Impact fractured samples of PC/ABS/PMMA blend were observed using SEM. An overview of the specimens shows that PC/ABS 75/25 and PC/ABS + 5% PMMA fractured in ductile mode [Fig. 8(a,b)]. This statement can be confirmed by a closer inspection of the fracture surfaces at higher magnifications from which rubber cavitation in ABS and shear yielding are revealed as the most important deformation processes during fracture [Fig. 9a,b]. In the case of PC/ABS + 10% PMMA, a ductile-to-brittle transition is observed; one half of the specimens fractured in ductile mode [Fig. 8(c)], whereas the other half broke in brittle manner [Fig. 8(d)]. The ductile samples have a large stable crack that arrested before the fracture was complete [see for example Fig. 7(a)]. (Cooling the specimens in liquid nitrogen and breaking them at high impact speed enabled a stable crack to be revealed.) At higher contents of PMMA (10–50%) the fracture surface is brittle [Fig. 8(e,f)].

Let us now focus on the ductile-to-brittle transition observed in PC/ABS + 10% PMMA. The fracture process can be divided into two parts: a) the crack initiation stage and b) the crack propagation stage. Ductile specimens present a large stable crack [Fig. 8(c)], where the crack initiation stage merges into the stable crack propagation stage, without a clear distinction. Enlarged views indicate that the movement of the crack front was followed by shear yielding and cavitating of rubber particles [Fig. 9(c)]. In contrast, the brittle specimens have a reduced crack initiation part (narrowed to 200 μm), at the end of which the crack continues to propagate in an unstable manner [Fig. 8(d)]. Crack initiation seems to be driven by a combination of craze formation and shear yielding. As the crack starts to propagate unstably, multiple crazing in a large volume of the material makes the fracture surface rough [Fig. 9(d)]. Since cavitation of rubber particles was observed in both ductile and brittle mode, the stresses required for rubber cavitation were much lower than for crazing or shear yielding, which is in good agreement with the observations of Kim.[24] Rubber cavitation was always observed during loading before crazes or a shear band started to grow. In addition, ductile fractured specimens were delaminated [Fig. 8(a–c)]. The delamination probably took place at the SAN/PC interface. This phenomenon has already been reported in the literature.[25] A large amount of energy is dissipated during this process, so delaminating contributes to the toughening of PC/ABS.

Moreover, when the content of PMMA is increased to 25% the crack initiation part decreases to approximately 25 μm [Fig. 8(e)], only a slight notch tip blunting can be observed [Fig. 8(f)], and the surface of the propagating part is much rougher. At 50% of PMMA the stability completely disappears. In the propagation stage large spots were visible, where the crack progressed easily without causing any plastic deformation [Fig. 9(f)]. It is likely that these were PMMA-rich phases, giving rise to brittle failure. The cracks in PMMA were initiated at

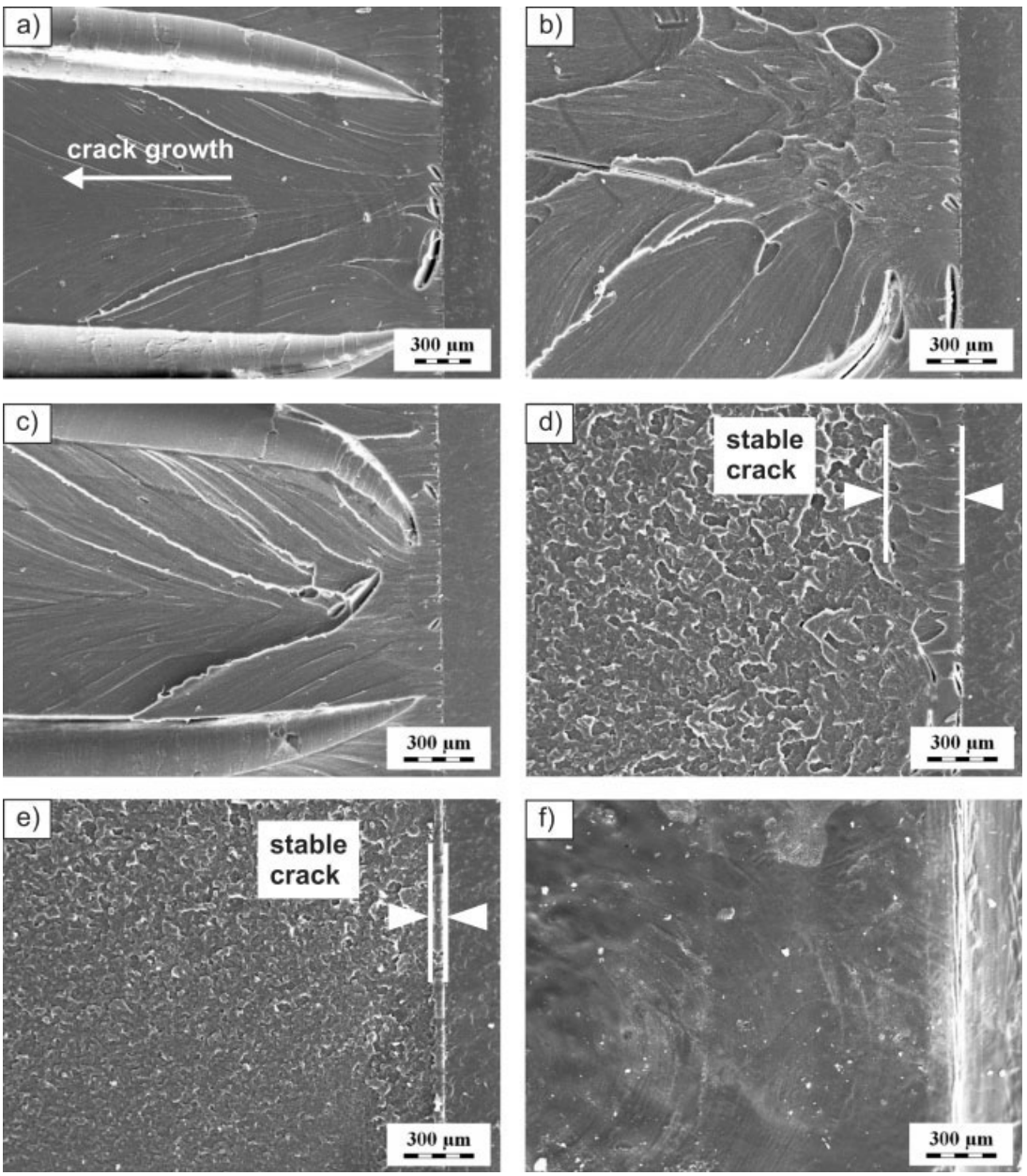

Figure 8 Fracture surface of PC/ABS/PMMA blend, crack development: (a) 0% PMMA; (b) 5% PMMA; (c) 10% PMMA ductile mode; (d) 10% PMMA brittle mode; (e) 25% PMMA; (f) 50% PMMA.

lower stresses, transiting quickly through the material, and they were slowed down by local plastic deformation of the PC/ABS domains surrounding PMMA. Since ABS is a minor phase in this blend, rubber cavitations were less frequent.

Phase structure analysis

Although PMMA is partially miscible with both ABS[26–30] and PC,[31,32] upon melt mixing a phase separation occurs.[33–36] In the binary blends of ABS/PMMA 75/25 [Fig. 10(a)] and PC/PMMA 75/25 [Fig. 10(b)], the PMMA phase forms a dispersed morphology and copies the shape of the melt flow patterns. (The melt flow patterns are typical of injection molding. They are generated by a speed/shear profile and are perpendicular to the melt flow direction. The gradient is highest near the walls of the injection mold.) The PMMA seems to be better dispersed in PC than in ABS. Finer PMMA dispersion in PC matrix is a result of the higher shear rates developed during melt mixing, due to the greater viscosity difference that exists between PC and PMMA than between ABS and PMMA. Furthermore, in certain melt flow patterns, where less intense mixing has taken place, PMMA phase forms large

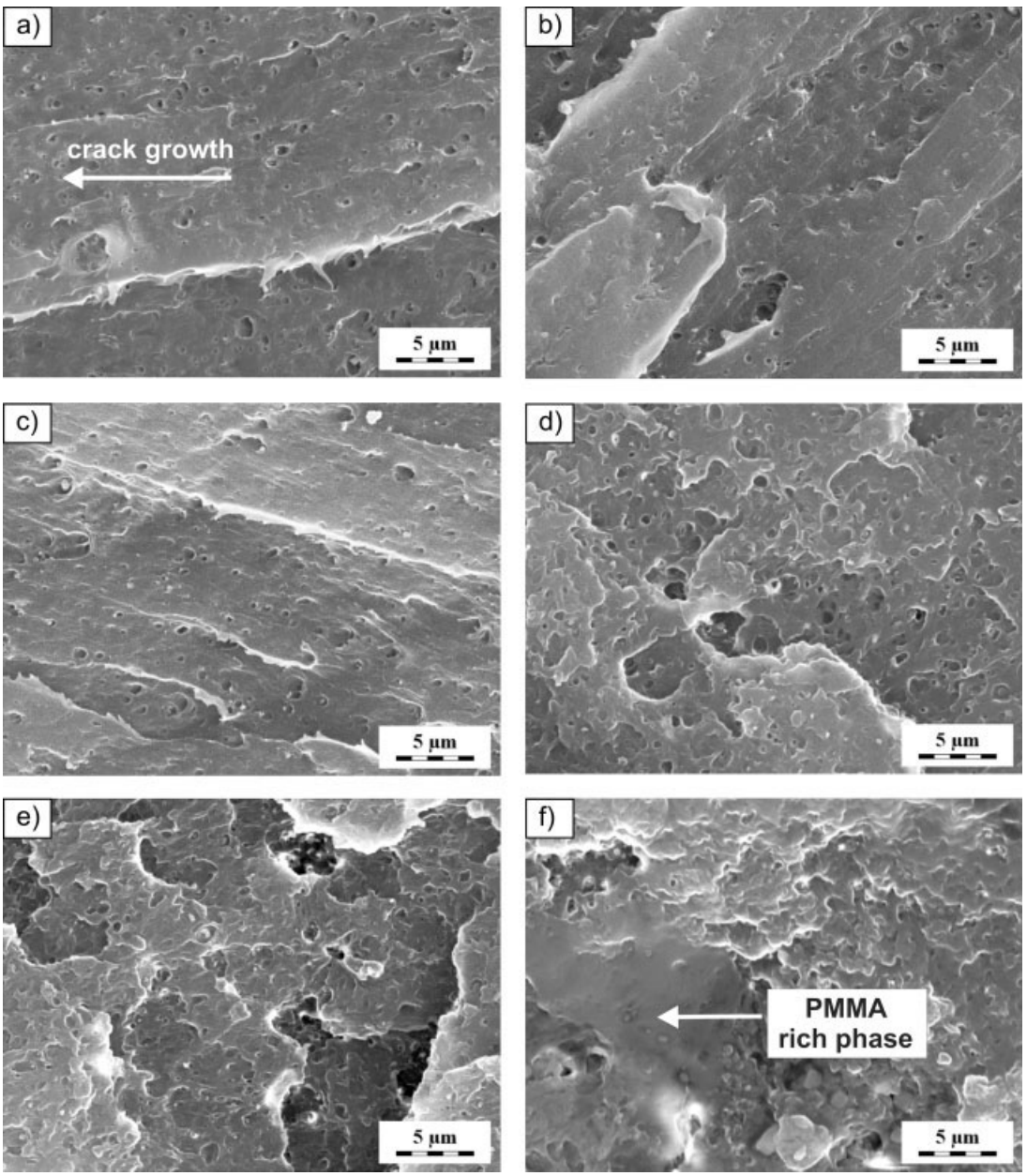

Figure 9 Fracture surface of PC/ABS/PMMA blend, crack propagation: (a) 0% PMMA; (b) 5% PMMA; (c) 10% PMMA ductile mode; (d) 10% PMMA brittle mode; (e) 25% PMMA; (f) 50% PMMA.

domains with PC [Fig. 10(b)]. Such structures may therefore be considered as a local inhomogeneity. On the other hand, PC/ABS 75/25 exhibits fine dispersion of ABS in PC [Fig. 10(c)]. Obviously, the rubber particles are distributed within the SAN phase. Again, it is apparent in some melt flow patterns that the ABS phase is enlarged. In this way a local continuous PC/SAN interface was created. Subsequently, during the impact test, the interface delaminates, as was shown above in the fracture surface images [Fig. 10(a–c)].

Figure 11 presents the morphology of PC/ABS/PMMA blend. The sample containing 5% of PMMA shows fine dispersion of ABS in PC matrix [Fig. 11(a)], promoting high toughness of the blend. As the content of PMMA increases up to 10%, elongated particles of PMMA emerge [Figs. 11(b), 12(a)]. Marin et al.,[33] based on immiscible rich phases weight calculations, reported the existence of a single PC-rich phase for the 0–12% total PMMA range, and the coexistence of both a PC-rich phase and a PMMA-rich phase for the 12–90% total PMMA range. The miscibility was shown to be dependent on the PC/PMMA molecular weight ratio.[33,37] ABS and PMMA are also partially miscible, the ABS/PMMA interfacial tension is even lower than that of PC/PMMA,[38]

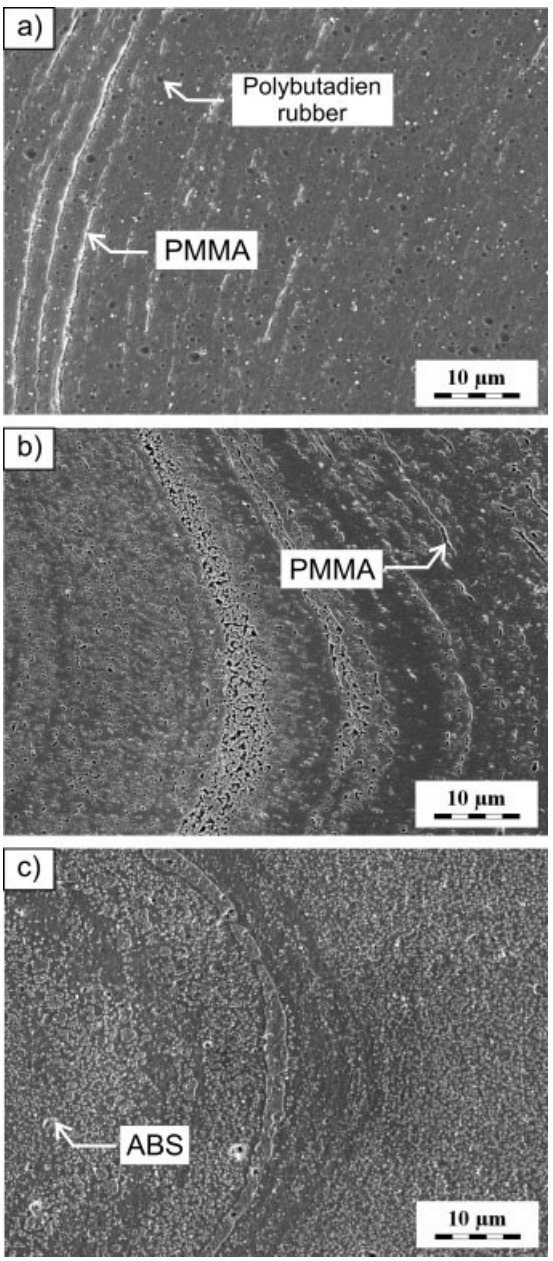

Figure 10 Morphology of binary blends: (a) ABS/PMMA 75/25; (b) PC/PMMA 75/25; (c) PC/ABS 75/25.

but ABS/PMMA also tend to phase-separate, depending on AN level.[29] Therefore, the amount of homogeneously dissolved PMMA in ABS and PC is questionable at the present time. Furthermore, the large inhomogeneities of PMMA are probably developed due to insufficient mixing of the blend in the injection molding unit. The transition may then occur when a critical number of inhomogeneities are present in the blend (especially at the fracture cross section). Embrittlement is usually attributed to stress concentration in the hard dispersed phase, giving rise to secondary crack formation. However, in our case, we can observe rather the change in the fracture mechanism, i.e., from shear yielding to multiple-crazing [compare Fig. 9(c,d)]. Thus, it is also possible that the transition arises as a result of morphology-induced stress state alternation. In PC/ABS blends, the ABS dispersed phase generates yielding of the PC matrix, if the PC matrix ligaments are thin enough. However, this is no longer valid when the ABS morphology transforms to cocontinuous. Then, the PC matrix ligaments become larger in size, and a local plain stress to plain strain transition takes place.[21] Moreover, Cheng et al.[38] have shown that the SAN (25% AN) dispersed phase was enlarged and tended toward cocontinuity with the PC phase when an impact modifier with a PMMA outer shell is added. This effect was considered to be a result of the partial miscibility of PMMA/SAN. Thus, such an enlargement of the SAN phase upon addition of PMMA can also be anticipated in our case. Now, looking at the morphology of PC/ABS/PMMA blend (Fig. 11) we can see that the structure becomes coarser upon addition of PMMA. The coarsening of the structure is more evident when there are higher concentrations of PMMA (25%, 50%) [Fig. 11(d,e)]. (To distinguish single phases the etching agent was selected in such a way that it reacts most strongly with PMMA, leaving deep cavities in the surface. On the other hand, the highest peaks are of SAN origin. Polybutadiene rubber and PC react intermediately with the etching agent.) The magnified view of the composition with 50% of PMMA [Fig. 12(b,c)] shows that PMMA and PC locally create a cocontinuous morphology [Fig. 12(c1)], and ABS is either dispersed in PC, or it resides on the PC/PMMA interface [Fig. 12(c2)]. In this way the area of the PC/ABS interface, and also the dispersion of ABS in PC, are greatly reduced, so the toughening effects are hindered. However, it is important to remember here that the ternary blend of PC/ABS + 50% PMMA still has higher impact toughness than the binary blend of PC/PMMA(50/50) or ABS/PMMA(50/50) blend. In other words, the toughening mechanisms of PC/ABS still function in this PMMA-rich ternary composition, which was well seen on the fracture surfaces, where the brittle PMMA-rich particles were surrounded by local plastically deformed material [see Fig. 9(f)].

On the whole, it follows from the facts mentioned above that the inhomogeneities of PMMA, which can develop when there is insufficient mixing of the blend in the injection molding unit, will reduce the toughness of the blend. The ductile-to-brittle transition occurs when a critical number of inhomogeneities are present in the blend. Furthermore, less dispersion of ABS in PC, leading to coarsening of the PC/ABS structure when there is approximately a 10% content of PMMA, also contributes to the ductile-to-brittle transition.

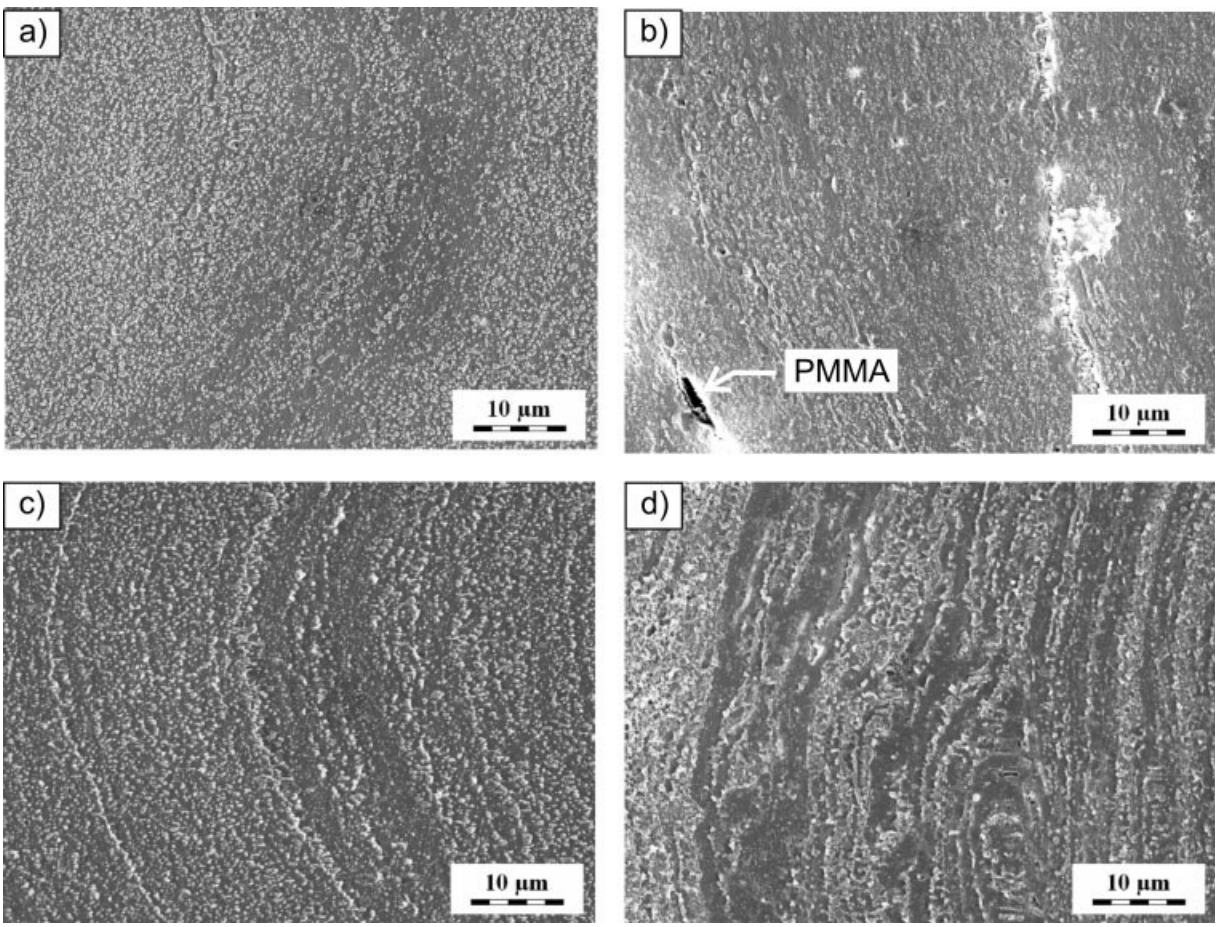

Figure 11 Morphology of PC/ABS/PMMA blend: (a) 5% PMMA; (b) 10% PMMA; (c) 25% PMMA; (d) 50% PMMA.

Effect of recycling

As had been anticipated, reprocessing affects the toughness of the materials studied here. In general, the loss of properties is associated with a decrease in the molecular weight of PC,[39–45] SAN[46] and thermo-oxidative degradation of butadiene rubber in the case of ABS or PC/ABS.[47] The *J* values of recycled PC/ABS blend declined by 10%. However, it is important to note that the toughness was higher than that of the commercial blend Cycoloy HF1100, GE Plastics (compare materials 1, 2, 3 in Fig. 13). Moreover, processing a ternary blend PC/ABS + 5% PMMA from virgin and recycled materials does not lead to any recognizable change in toughness (compare materials 3, 4 in Fig. 13). Additionally, the content of 2% of TPE in the PC/ABS/PMMA5 resulted in a drop in toughness of almost 40%. However, despite this effect, the *J* value lies at the same level as that for virgin PC, ABS, and PMMA (compare materials 6, 7, 8, 9 in Fig. 13).

Tensile testing reveals that the addition of 5% of PMMA increases the yield stress σ_y of PC/ABS blend (compare materials 4, 5 in Fig. 14). The yield stress σ_y and strain ε_y of virgin and recycled ternary blend PC/ABS + 5% PMMA remain almost unchanged (compare materials 5, 6 in Fig. 14). Moreover, the addition of TPE does not affect the deformation behavior and the material is competitive with original materials (compare materials 1, 2, 3, 7 in Fig. 14). Recycling decreases the tensile strain at break (not shown here), but this is not crucial for safe engineering design.

Rheological behavior

The viscosity versus shear rate plot for PC, ABS, and PMMA at 250°C is given in Figure 15. In general, the plots indicate a decrease in viscosity with increasing shear rate, which is a characteristic behavior of non-Newtonian shear thinning fluids. Common shear rates during processing of polymer melts by injection molding are in the range of 10^1–10^3 1/s. Figure 15 shows constant viscosity of PC, which starts to decrease at higher shear rates. By contrast, the viscosity of ABS and PMMA declines continuously with shear rate, and reveals identical melt flow behavior for these two materials. Furthermore, the viscosity of the PC/ABS blend is lower than that of

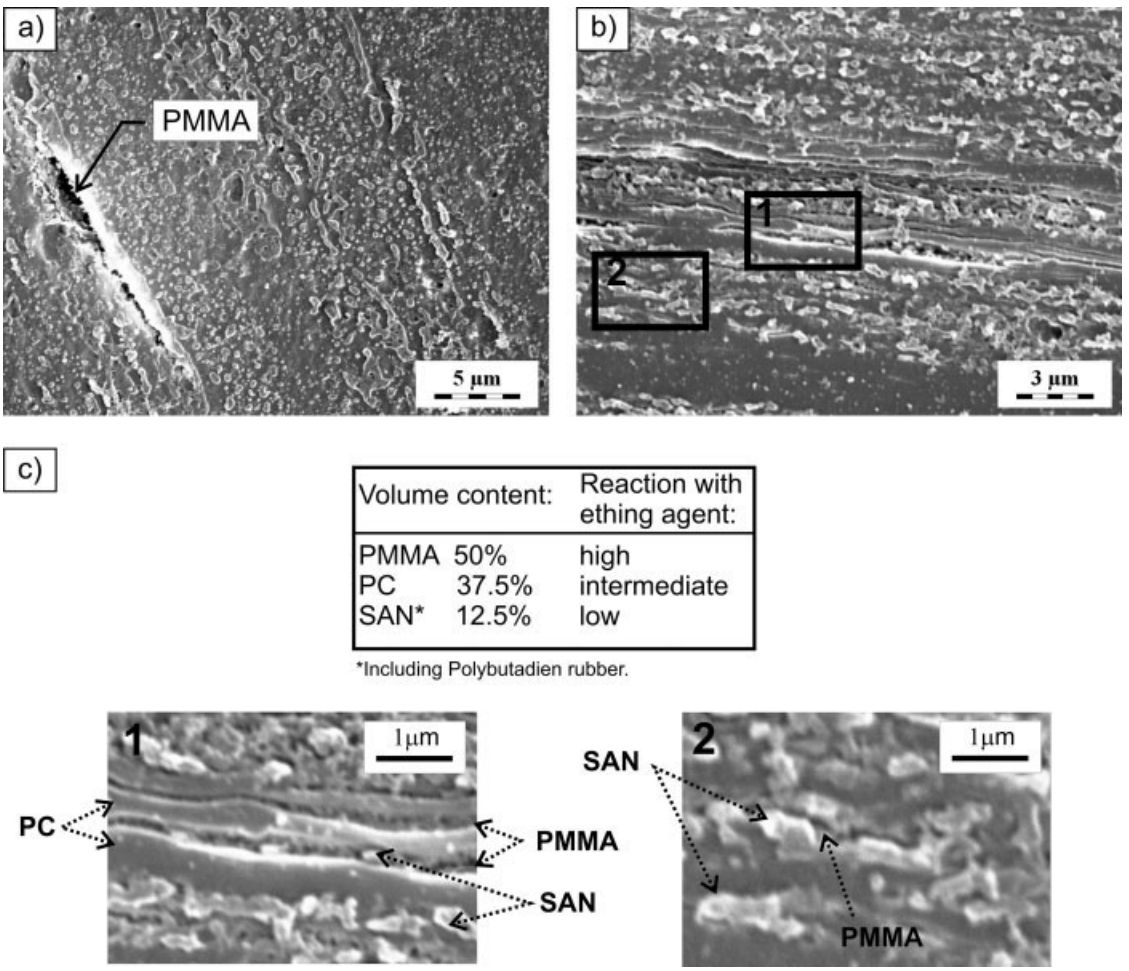

Figure 12 Detailed view of etched morphology of PC/ABS/PMMA blend: (a) 10% PMMA; (b) 50% PMMA; (c) Section view of the image (b).

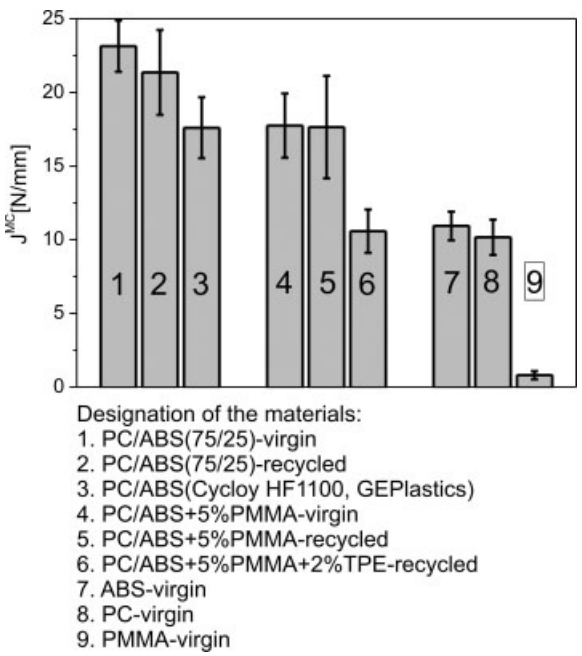

Figure 13 The effect of recycling on toughness.

pure PC and ABS. The decrease in viscosity at constant shear rates of 10^1–10^3 1/s upon addition of ABS is well documented in Figure 16. This negative blending effect for PC/ABS prepared by melt mixing has already been reported in the literature,[48] where it was attributed to three possible causes: (1) plasticisation; (2) degradation of PC by metal salts present in ABS[49,50]; and (3) poor interfacial interaction. The first and third factors contradict our findings, in as much as blending had a positive impact on the mechanical properties. On the other hand, we have observed a strong temperature dependence of blend toughness, which supports the idea of chemical reactions deteriorating the PC phase during melt mixing. Additionally, the effect of PMMA on PC/ABS blend is shown in Figure 17. The viscosity at constant shear rates at 250°C exhibits a moderate linear decrease upon addition of PMMA, which is especially evident at higher shear rates. It can be concluded that even 5% of PMMA improves the processability of the blend. On the whole, the key information for practical applications is that the PC/

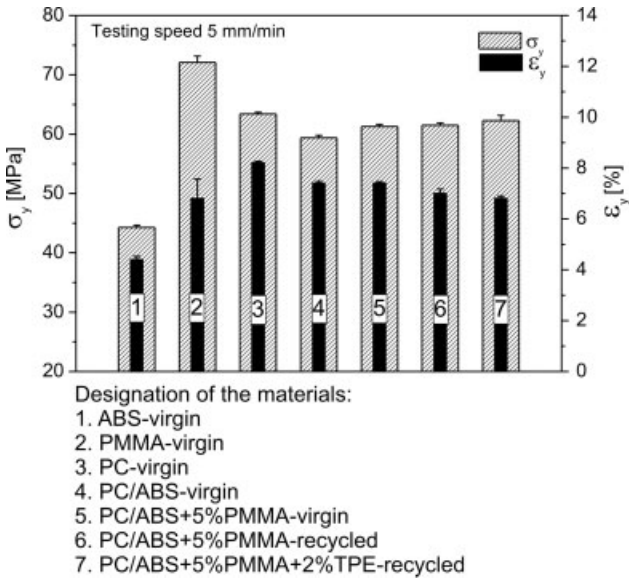

Figure 14 The effect of recycling on tensile properties.

ABS/PMMA blends show excellent processability, which increases with the addition of ABS and PMMA.

CONCLUSIONS

This work has characterized the toughness of binary and ternary blends based on PC, ABS, and PMMA. In the ternary PC/ABS/PMMA blend a ductile-to-brittle transition was found at 10% of PMMA, where the fracture behavior changed from ductile elastic-plastic to brittle linear-elastic. Fracture surfaces analysis showed that the ductile-to-brittle transition was accompanied by a reduction in the crack initiation part, followed by rapid—unstable—crack propagation. Crack initiation and propagation was driven by a combination of shear yielding and craze formation, the latter being dominant when PMMA was added.

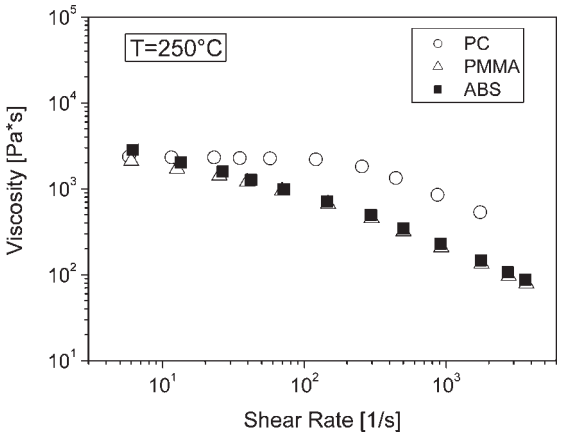

Figure 15 Rheology results of PC, ABS and PMMA.

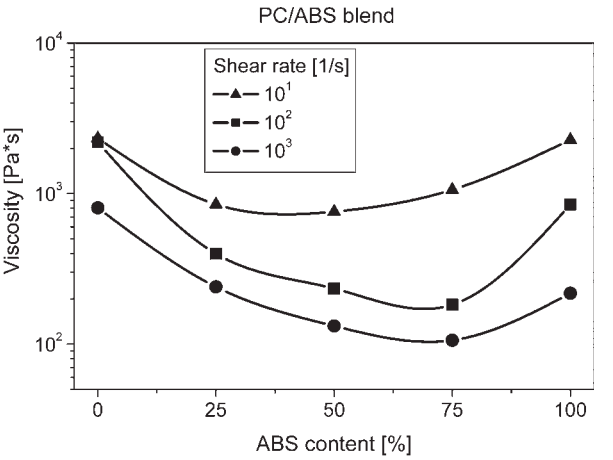

Figure 16 Rheology results of PC/ABS blend.

Cavitation of rubber particles was observable even at 50% of PMMA. Morphology investigations showed that inhomogeneities of PMMA, which can develop when there is insufficient mixing of the blend in the injection molding unit, reduce the toughness of the PC/ABS/PMMA blend. The ductile-to-brittle transition presumably occurs when a critical number of inhomogeneities are present in the blend. Furthermore, less dispersion of ABS in PC, leading to coarsening of the PC/ABS structure when the content of PMMA is about 10%, also contributes to the ductile-to-brittle transition. Recycling had only a slight effect on dynamic fracture toughness and tensile properties. The yield stress and strain remains almost unchanged when compared with the blend produced from original materials. Recycling decreases the tensile strain at break, but this is not crucial for safe engineering design. The rheological properties demonstrated that the ternary blend can be well processed under injection molding conditions. Essentially, ABS and PMMA improved processability.

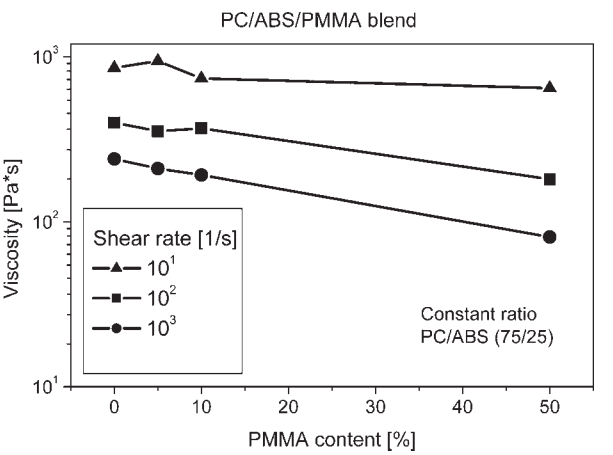

Figure 17 Rheology results of PC/ABS/PMMA blend.

Recycled blends were shown to have competitive mechanical properties in comparison to original materials. Especially the ternary blend compositions PC/ABS 75/25 containing less than 10% PMMA exhibited superior toughness to that of pure original materials. The toughness depended strongly on the processing temperature. It can be recommended that thermomechanical loading of the molten material be kept as low as possible.

References

1. Jenseit, W.; Stahl, H.; Wollny, V.; Wittlinger, R. Recovery Options for Plastics Parts from End-of-Life Vehicles: An Efficiency Assessment, Final Report; Öko-Institut e.V.: Darmstadt, 2003.
2. Fisch, H. In Plastics Impact on the Environment, Proceedings of the Global Plastics Environmental Conference (GPEC) 2003; Society of Plastics Engineers (SPE): Detroit, 2003; p 117.
3. Hähnsen, H.; Kranz, G.; Opelka, G.; Orth, P.; Sandquist A. Kunststoffe 1996, 86, 1172.
4. Schlotter, U. Kunststoffe 1996, 96, 1084.
5. Fraunholcz, N.; Campen, N.; van Schurr, S. U. In Proceedings of International Automobile Recycling Congress, Geneva 2003.
6. Liu, X.; Berlitson, H. J Appl Polym Sci 1999, 74, 510.
7. Klason, C.; Bertilsson, H.; Liu, X. Makromol Chem Macromol Symp 1998, 135, 183.
8. Liang, R.; Gupta, R. K.; In Proceedings of Annual Technical Conference (ANTEC) 2002—Plastics; Society of Plastics Engineers (SPE). San Francisco 2002, Vol 3, p 2948.
9. Elmaghor, F.; Zhang, L.; Fan, R.; Li, H. Polymer 2004, 45, 6719.
10. Balart, R.; López, J.; García, D; Salvador, M. D. Eur Polym Mater 2005, 41, 2150.
11. Fisher, J. D. U.S. Pat. 5,232,986 (1993).
12. Lieberman, M. U.S. Pat. 5,569,713 (1996).
13. Woei-Min, T. U.S. Pat. US 2,004,209,985 (2004).
14. Grellmann, W.; Seidler, S., Eds. Deformation and Fracture Behaviour of Polymers; Springer Verlag: Berlin Heidelberg, 2001.
15. Grellmann W. Lach, R. Appl Macromol Chem Phys 1997, 253, 27.
16. Han, Y.; Lach, R.; Grellmann, W. J Appl Polym Sci 2001, 79, 9.
17. Merkle, J. G.; Corten, H. T. J Press Vessel Technol 1974, 96, 286.
18. Kobayashi, T. Eng Fract Mech 1984, 19, 67.
19. Hoffmann, H.; Grellmann, W.; Zilvar, V. In Proceedings of 28th Microsymposium on Macromolecules Prague 1985, Polymer Composites; Walter de Gruyter: Berlin, 1986; p 232.
20. Grellmann, W.; Jungbluth, M. In Fracture Mechanics, Micromechanics and Coupled Fields (FMC)-Series, No. 37; Institut für Mechanik: Berlin Chemnitz, 1987; p 186.
21. Greco, R.; Sorrentino, A. Adv Polym Tech 1994, 13, 249.
22. Lee, M. P.; Hiltner, A.; Baer, E. Polym Eng Sci 1992, 32, 909.
23. Lombardo, B. S.; Keskkula, H.; Paul, D. R. J Appl Polym Sci 1994, 54, 1697.
24. Laatsch, J.; Kim, G. M.; Michler, G. H.; Arndt, T.; Süfke, T. Polym Adv Technol 1998, 9, 716.
25. Inberg, J. P. F.; Gaymans, R. J Polymer 2002, 43, 2425.
26. Kim, W. N.; Burns, C. M. J Appl Polym Sci 1990, 41, 1575.
27. Fowler, M. E.; Keskkula, H.; Paul, D. R. Polymer 1987, 28, 1703.
28. Fowler, M. E.; Barlow, J. W.; Paul, D. R. Polymer 1987, 28, 2145.
29. Fowler, M. E.; Barlow, J. W.; Paul, D. R. Polymer 1987, 28, 1177.
30. Wen, G.; Li, X.; Liao, Y.; An, Y. Polymer 2003, 44, 4035.
31. Chiou, J. S.; Barlow, J. W.; Paul, D. R. J Polym Sci Polym Phys 1987, B25, 1459.
32. Keitz, J. D.; Barlow, J. W.; Paul, D. R. J Appl Polym Sci 1984, 29, 3131.
33. Marin, N.; Favis, B. D. Polymer 2002, 43, 4723.
34. Kim, B. K.; Yoon, L. K.; Xie, X. M. J Appl Polym Sci 1997, 66, 1531.
35. Haufe, A.; Menning, G.; Hellmann, P. Plastics, Rubber and Composites Processing and Applications 1994, 22, 277.
36. Li, Q.; Tian, M.; Kim, D.; Zhang, L.; Jin, R. J Appl Polym Sci 2002, 85, 2652.
37. Akkapeddi, M. K.; In Polymer Blends Handbook; Utracki, L. A., Ed.; Kluwer Academic Publishers: Dordrecht, 2002; Vol. 2, Chapter 15, p 1023.
38. Cheng, T. W.; Keskkula, H.; Paul, D. R. Polymer 1992, 33, 1606.
39. Liu, Z. Q.; Cunha, A. M.; Yi, X. S.; Bernardo, A. C. J Appl Polym Sci 2000, 77, 1393.
40. Abbas, K. B. Polym Eng Sci 1980, 20, 376.
41. Bernardo, C. A. In Frontiers in the Science and Technology of Polymer Recycling; Akovali, G., Ed.; Kluwer Academic Publishers: London, 1998; Chapter 3, p 215.
42. La Mantia, F. P.; In Frontiers in the Science and Technology of Polymer Recycling; Akovali, G., Ed.; Kluwer Academic Publishers: London, 1998; Chapter 3, p 249.
43. Shea, J. W.; Aloisio, C.; Cammons, R. R. In Proceedings of Annual Technical Conference (ANTEC) 1975, p 614.
44. Bledzki, A. K.; Barth, C.; Hähnsen, H.; Orth, P. Kunstst Plast Eur 1997, 87, 1124.
45. Rybnicek, J. Diploma Thesis, Czech Technical University, Prague, 2001.
46. Bastida, S.; Marieta, C.; Eguiazabal, J. I.; Nazabal, J. Eur Polym Mater 1995, 31, 643.
47. Eguiazábal, J. I.; Nazábal. J Polym Eng Sci 1990, 30, 527.
48. Balakrishnan, S.; Neelakantan, N. R.; Nabi Saheb, D.; Jog, J. P. Polymer 1998, 39, 5765.
49. Lee, M. S.; Kao, H. C.; Chiang, C.; Su, D. T. In Polymer Blends and Alloys; Kohudic, M. A., Ed.; Technomic Publishing Company: Pennsylvania, 1988; p 25.
50. Chin, W. K.; Hwang, J. L. In Polymer Blends and Alloys; Kohudic, M. A., Ed.; Technomic Publishing Company: Pennsylvania, 1988, p 154.